IJNRD.ORG ISSN : 2456-4184
INTERNATIONAL JOURNAL OF NOVEL RESEARCH AND DEVELOPMENT (IJNRD) | IJNRD.ORG
An International Open Access, Peer-reviewed, Refereed Journal

Crop growth monitoring by dual polarimetric radar vegetation index (DpRVI) using Sentinel-1 SAR data for the soybean crop in Latur District of Maharashtra

Gargi Gaydhane[a], Upasana Singh[b], Ashutosh Pawar[c]
a,b,c Semantic Technologies and Agritech Services Private Limited, Pune

Abstract

The utilization of Sentinel-1 Synthetic Aperture Radar (SAR) satellite data offers an exceptional opportunity for crop growth monitoring due to its better revisit frequency and extensive spatial coverage. This study leverages Sentinel-1 SAR data, specifically the dual-pol data comprising VV (Vertical-Vertical) polarization and VH (Vertical-Horizontal) polarization, to apply remote sensing and geospatial techniques in agriculture. These techniques harness Sentinel-derived information to support crop growth monitoring, particularly as an alternative to Sentinel 2A optical data, which can be hindered by cloud coverage. while previous literature has explored the use of backscatter data for crop characterization, this research takes a novel approach. It combines scattering information, including the degree of polarization and eigenvalue spectrum, to derive a new vegetation index known as the Dual Polarimetric Radar Vegetation Index (DpRVI) from dual-pol SAR data. This innovative index provides valuable insights into vegetation dynamics. Furthermore, this study focuses on assessing plant growth in the Bhada Revenue Circle, Latur district, Maharashtra. It does so by considering key crop biophysical parameters such as Plant Area Index (PAI), Vegetation Water Content (VWC), Normalized Difference Vegetation Index (NDVI), and Land Surface Water Index (LSWI) at various crop phenological growth stages. This approach allows for a comprehensive analysis of crop development throughout its lifecycle, emphasizing each critical growth stage. To validate the accuracy of these assessments, statistical analyses, including Linear regression, are employed. These analyses reveal correlations between each biophysical parameter and the Dual Polarimetric Radar Vegetation Index (DpRVI). These correlations provide valuable insights into Soybean crop performance, aiding in the prediction of crop yields and overall crop health. The study's findings indicate promising results for Soybean crop monitoring and highlight the potential of SAR data in agricultural applications.

Indeed, the accumulation of key biophysical parameters including Plant Area Index (PAI), Vegetation Water Content (VWC), Normalized Difference Vegetation Index (NDVI), and Land Surface Water Index (LSWI) plays a significant role in plant growth development. In this context, The Dual Polarimetric Radar Vegetation Index (DpRVI) is a useful monitoring plant development during the kharif season, when microwave data may be used instead of optical data. Its correlation with biophysical parameters like PAI, VWC, NDVI, LSWI enhances yield predictions and supports informed decision-making, improving agricultural productivity and crop management practices.

Keywords
Soybean, DpRVI, PAI, VWC, NDVI, LSWI, Dual Polarization

Aims and Objectives

1. Crop health monitoring of Soybean crop in the kharif season
2. Determination of crop condition with crop biophysical properties and their relationship between crop growth stages and vegetation dynamics using Sentinel 1 data

1.Introduction

In 2009 ESA launched an international AgriSAR field campaign, by this campaign frequent coverage from the C-band radar on Sentinel-1 could deliver essential information to improve agricultural practices which leads to crop growth monitoring and vegetation condition**.** The Sentinel-1 mission's dual-pol SAR dataset availability offers exceptional chances to expand operational monitoring for a number of application communities. (User guide ESA). Monitoring crop conditions is a key component of production estimation and forecasting. When organizations need to continuously monitor agricultural production over huge geographic areas, mapping from space is a practical solution. Despite the fact that optical remote sensing has been employed successfully (Boryan et al., 2011; de Wit et al., 2012; Lopez-Lozano et al., 2015; Chipanshi et al., 2015) must be restricted to almost cloud-free situations for useful acquisitions by this sort of sensor in numerous operational frameworks (for example, MODIS vegetation products). Due to the fact that synthetic aperture radar (SAR) systems can monitor in all-weather situations and that the microwave signal is sensitive to the dielectric and geometrical characteristics of crops, synthetic aperture radar (SAR) data are of great importance for agricultural applications in this context. (Ulaby, 1975; Mcnairn and Shang, 2016). Due to their wider swaths and smaller data volumes, dual-pol modes are preferable to full-pol acquisitions, but at the expense of their insufficient polarimetric information. (Lee et al., 2001; Ainsworth et al., 2009), providing certain advantages for organizations continuing operational processes. The Sentinel-1 dual-pol mode (VV-VH) describes the simultaneous reception of vertical and horizontal polarizations while transmitting a vertically polarised signal. As a result, backscatter intensities from the received wave in cross-polarized channels (VV-VH) reveal information about a target. The backscatter intensities were used in several investigations to identify different varieties of crops. (Kussul et al., 2016; Nguyen et al., 2016; Bargiel, 2017; Van Tricht et al., 2018; Mandal et al., 2018; Whelen and Siqueira, 2018; Arias et al., 2020) and crop biophysical parameter estimation (Bousbih et al., 2017; Kumar et al., 2018; Mandal et al., 2020). Due to the sensitivity of backscatter intensities to crop morphological and phenological development, crop monitoring methods based purely on scattering powers were developed. (Nelson et al., 2014; De Bernardis et al., 2015; Nguyen et al., 2016; Lasko et al., 2018; Singha et al., 2019; Fikriyah et al., 2019). Several research has investigated the derivation of vegetation metrics from SAR data using backscatter intensity ratios. (Blaes et al. 2006) growth dynamics of maize is investigated by the sensitivity of σVH0 /σVV0. At incidence angles of 35–45°, σVV0 /σVH0 was sensitive to plant growth until the leaf area index (LAI) and vegetation water content (VWC) reached 4.9 m2m−2) and 5.6 kg m−2, these parameters are applied to crop classification (McNairn et al., 2009; Inglada et al., 2016; Denize et al., 2019), phenology estimation (McNairn et al., 2018; Canisius et al., 2018), and vegetation characterization (Veloso et al., 2017; Vreugdenhil et al., 2018; Khabbazan et al., 2019). Veloso et al. (2017) noted that this ratio was relatively stable during the pre-cultivation stages and increased significantly at the tillering stages of cereal crops like wheat and barley. Besides, this ratio provided better separability among maize, soybean, and sunflower during their heading/flowering stages. In this research, we utilize and derived the dual-pol Sentinel-1 SAR data to dual-pol radar vegetation index (DpRVI) for crop condition monitoring. (D. Mandal, et al., 2020) To create this new index, the degree of polarization is employed along with the eigenvalue spectrum produced by the dual-pol covariance matrix's eigen-decomposition. Leaving out the backscatter intensities for the polarisation channel (Chang et al., 2018; Periasamy, 2018), DpRVI is a ranging and valuation between 0 and 1.

We Performed and assessed the plant growth variables, on the basis of performance of the DpRVI with the help of Croptech PRO mobile application powered by Semantic Technologies and Agritech Services Pune for the ground truth plots of soybean crop, we perform a comparison and analysis between DpRVI, PAI, VWC, NDVI, LSWI for the soybean crop. also, assess the temporal variations of Soybean crop with DpRVI and biophysical parameters including PAI, VWC, NDVI, LSWI.

2. Study area

Latur is a district located in the Indian state of Maharashtra, situated within the Marathwada region. The city of Latur serves as the district headquarters. This region is situated on the Harishchandra- Balaghat plateau, at an elevation of approximately 636 meters above mean sea level. Latur is positioned near the Maharashtra-Karnataka state border.

The climate in Latur exhibits a wide temperature range, with temperatures varying between 13 to 41 degrees Celsius (55 to 106 degrees Fahrenheit). The monthly rainfall in Latur can fluctuate significantly, ranging from 9.0 to 693 millimeters (0.35 to 27.28 inches). On average, Latur receives approximately 725 millimeters (28.5 inches) of rainfall annually.

In recent times, Latur has experienced the impacts of climate change. This includes extreme weather events such as heavy rainfall and hailstorms during the summer months.

Latur District primarily specializes in Soybean cultivation during the kharif season. Specifically, the Bhada Revenue Circle, situated in the Ausa Taluka of Latur district, serves as the study area. Bhada is also known for being a dominant region for Soybean cultivation, making it a key area of focus for agricultural research and monitoring.

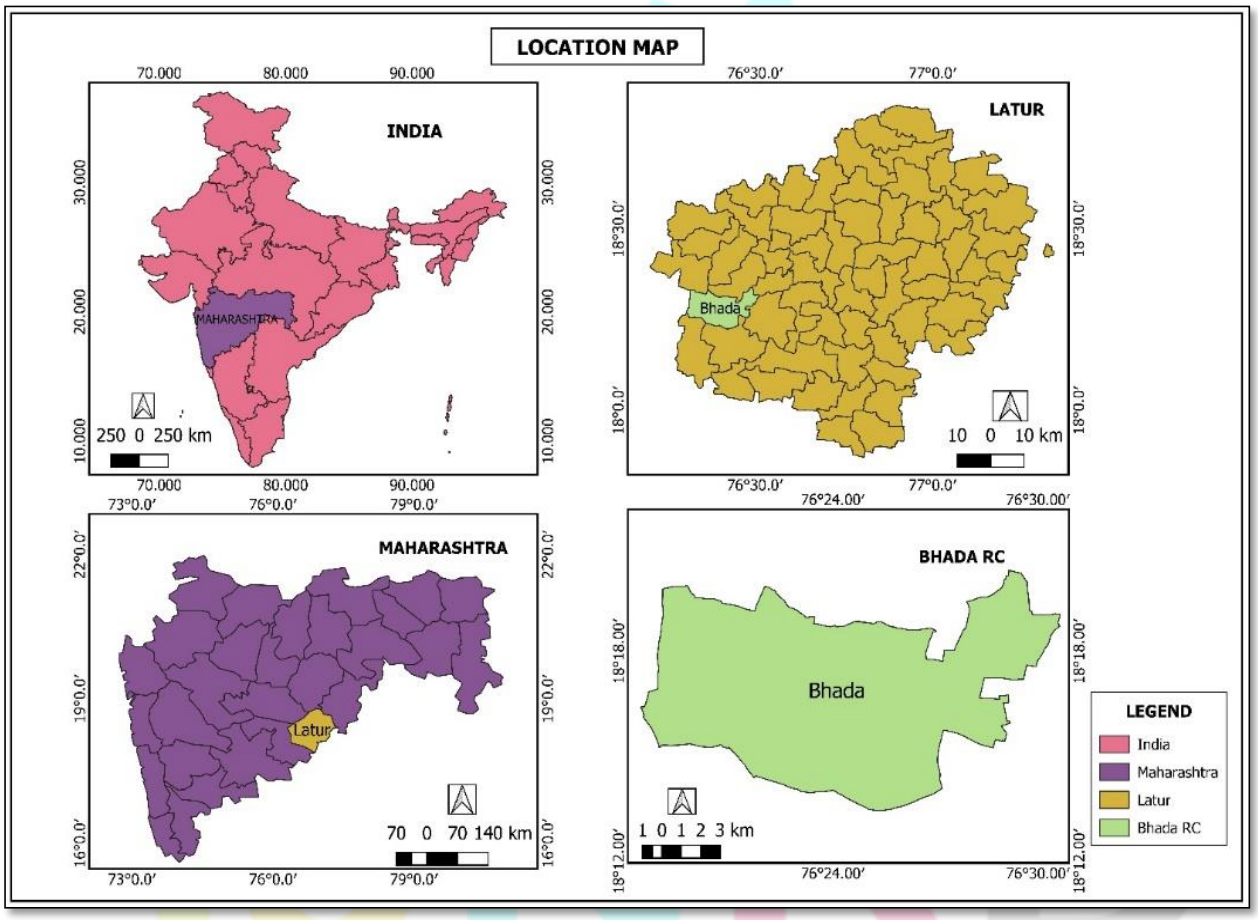

Fig 1: Location map of Bhada revenue circle in Latur district

3. Dataset

In this study data are as follows:

- Sentinel 1 SLC by ESA https://scihub.copernicus.eu/
- Sentinel 1 GRD by ESA https://scihub.copernicus.eu/
- Sentinel 2A by ESA https://scihub.copernicus.eu/
- MODIS by NASA https://modis.gsfc.nasa.gov
- Ground Truth Data using Croptech Pro mobile application by Semantic Technologies and Agritech Services Pune

In our current research, we focused on the Bhada revenue circle, which is known for its dominant Soybean crop cultivation. We adopted a systematic approach to sample 62 plots for Soybean analysis, following the principles

of the central limit theorem. These selected plots were registered and meticulously monitored using the Croptech Pro mobile application. This application provided us with valuable ground truth data, ensuring the accuracy and reliability of our study.

To monitor the crop growth at various phenological stages using the DpRVI, we relied on Sentinel-1 data. Specifically, we used Sentinel-1 Single Look Complex (SLC) data for crop classification purposes. Additionally, we utilized Sentinel-1 Ground Range Detected (GRD) data with VH polarization, which provided us with essential information for our research.

This comprehensive approach allowed us to assess and monitor Soybean crop growth in the Bhada revenue circle, enhancing our understanding of the crop's development and health throughout its lifecycle.

4. Methodology

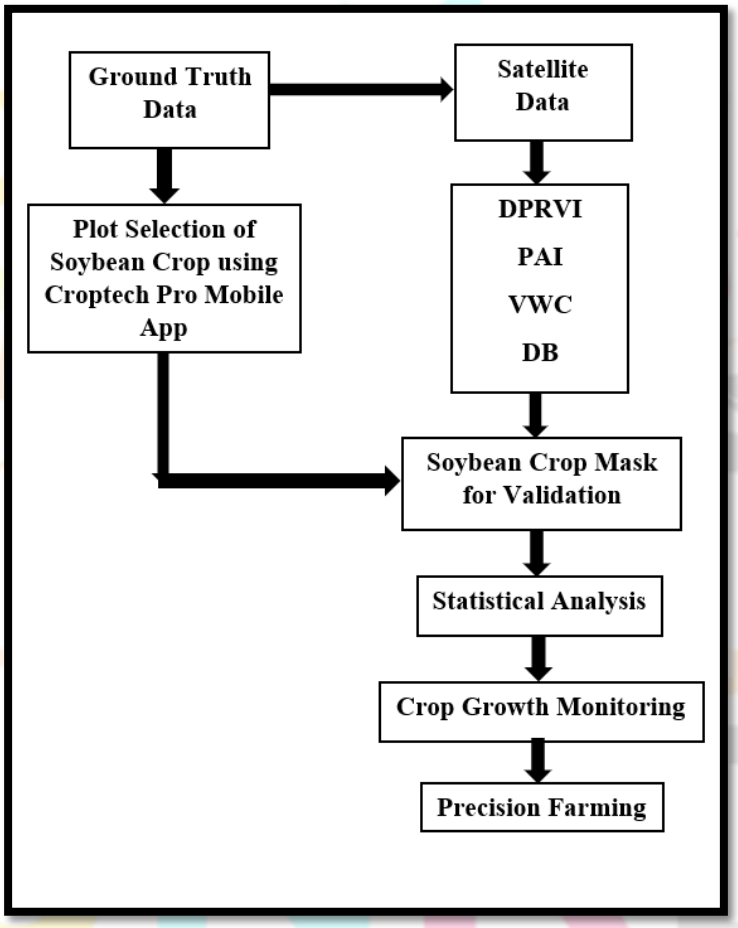

Fig 2: Methodology for overall research

4.1 SAR data preprocessing

In this study, we conducted various procedures on SAR data using the SNAP 9.0 Software. We utilized Sentinel 1-SLC multitemporal images, starting with the first image that was processed into TOPSAR split with the Interferometric Wide (IW) sub-swath product. We selected Bursts 3 to 7 out of a total of 9 Bursts and opted for both VV and VH polarizations. The IW swath comprises three sub-swaths: IW1, IW2, and IW3 in the range direction. Next, we applied the orbit file with a polynomial degree for radiometric calibration, selecting all the source bands in the processing parameters. The output was saved as a complex output, as complex values were necessary to generate the covariance matrix in subsequent steps.

Following this, we proceeded with the S-1 TOPSAR Deburst operation, selecting VV and VH polarizations in the processing parameters. Subsequently, we performed a subset operation in the UTM projected coordinate system

for the study area. Moving forward, we conducted Multilooking with a selection of all bands and generated the PolSAR matrix (C2). We selected C2 in the Polarimetric Matrix in the processing parameters. It's worth noting that all these steps were carried out using SNAP 9.0, a tool provided by ESA for processing Sentinel-1 images.

Once the C2 matrix/band was generated, we applied a polarimetric speckle filter. In the processing parameters, we selected the refined Lee filter with a window size of 5x5. We continued by specifying a number of looks as 1.

Subsequently, we proceeded with the range doppler terrain correction, selecting all source bands and sub-pixel accuracy with SRTM 3-Second data. The geocoded image was projected using the UTM Zone 43N projection in the processing parameters, and the default output was saved in BEAM DIMAP format.

For further analysis, each matrix element (C11, C22, C12, and C21) was stored individually in a binary format along with separate header information. DpRVI was then generated from the covariance matrix elements for each date. The DpRVI output was exported in GeoTIFF format for subsequent analysis, which included comparison with field and ground truth data.

There are two types of processing for SAR data which are as follows:

1) Single-date Processing

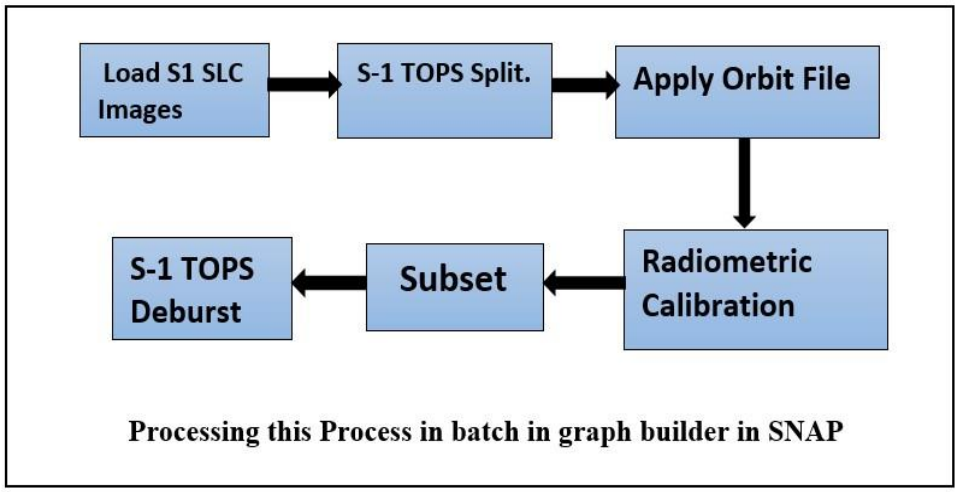

Fig 3. Processing flow chart for Sentinel 1 data

2) Multi-date Processing

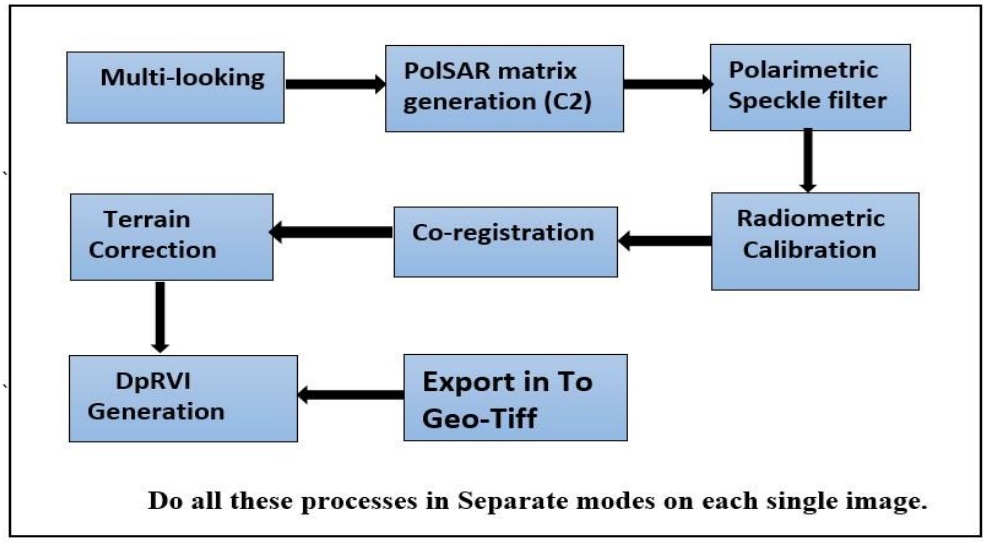

Fig 4. Processing flow chart for Sentinel 1 data

4.2 Dual-pol Radar Vegetation Index (DpRVI)

Information about spatial and temporal variations in crop growth and changes in their phenology growth stages provided by radar backscatter intensity (Lopez-Sanchez et al., 2014). SAR indices give a good physical interpretable vegetation descriptor that we can use for vegetation monitoring. Dual-pol-based vegetation index using Sentinel-1 data would be advantageous for operational crop monitoring over fields. (D. Mandal et.al, 2020) for calculating the DpRVI degree of polarization and the eigenvalue spectrum to derive a new vegetation index from dual-pol SAR data. The equation mentioned below explains the mechanism of DpRVI.

The equation and mechanism in DpRVI are explained as follows:

DpRVI is calculated from dual-pol 2x2 covariance matric C2.

$$C2 = \begin{bmatrix} C11 & C12 \\ C21 & C22 \end{bmatrix} = \begin{bmatrix} (|Svv|) & (S * vh) \\ (SvhSvv) & (|Svh|2) \end{bmatrix} \qquad (1)$$

The scattering information in terms of the degree of polarization and the eigenvalue spectrum is jointly utilized to derive the vegetation index from dual-pol SAR data. The state of polarization of an EM wave is characterized in terms of the degree of polarization (m) as proposed by Barakat (1977):

$$m = \sqrt{1 - \frac{4|C2|}{(Tr(C2))2}} \qquad (2)$$

where Tr is the matrix trace operator (i.e., the sum of the diagonal elements) and |.| is the determinant of a matrix.

The two non-negative eigenvalues ($\lambda 1 >= \lambda 2 >= 0$) are obtained from the eigen-decomposition of the C2 matrix which is then normalized with the total power Span ($Tr(C^2) = \lambda 1 + \lambda 2$). The eigenvalues quantify the dominance of scattering mechanisms. Hence, the parameter beta is introduced as beta = lambda1/Span

The dominant scattering information is modulated with the degree of polarization (m), which in particular characterizes anisotropy for dual-pol SAR data. The scattering randomness is then obtained by subtracting m x beta from unity, as given in the following equation by (Mandal et al. 2020), and user guide SNAP Software.

$$\mathbf{DpRVI} = 1 - m\beta, \; 0 \leq \mathbf{DpRVI} \leq 1 \qquad (3)$$

Plant structural heterogeneity throughout the Sentinel-1 pre-processing phase for time-series data. reproductive to maturity stage may result in spatial variation within a parcel. as a result, at advanced development stages, the deviation in DpRVI values from the mean may rise.

(Mandal D., et al. 2020)

The standard deviation of λ1/Span is lower than that of λ2/Span, and the mean value decreases with the plant growth stage. As a result, the product of m and corresponds to the dominating scattering scaling. As the crop canopy develops, the order of scattering increases. during the early stages of crop development (early leaf development), scattering from the soil surface is typically dominant. However, multiple scattering from the canopy and soil is more visible at the advanced vegetative stage. As a result, m is projected to decrease from the early to the mature vegetative stage. It should be observed that as the order of scattering increases, so does the sensitivity of the degree of polarization. (Mandal, D., et al. 2020)

The main reason for coupling m and β is their differential sensitivity to crop growth dynamics.

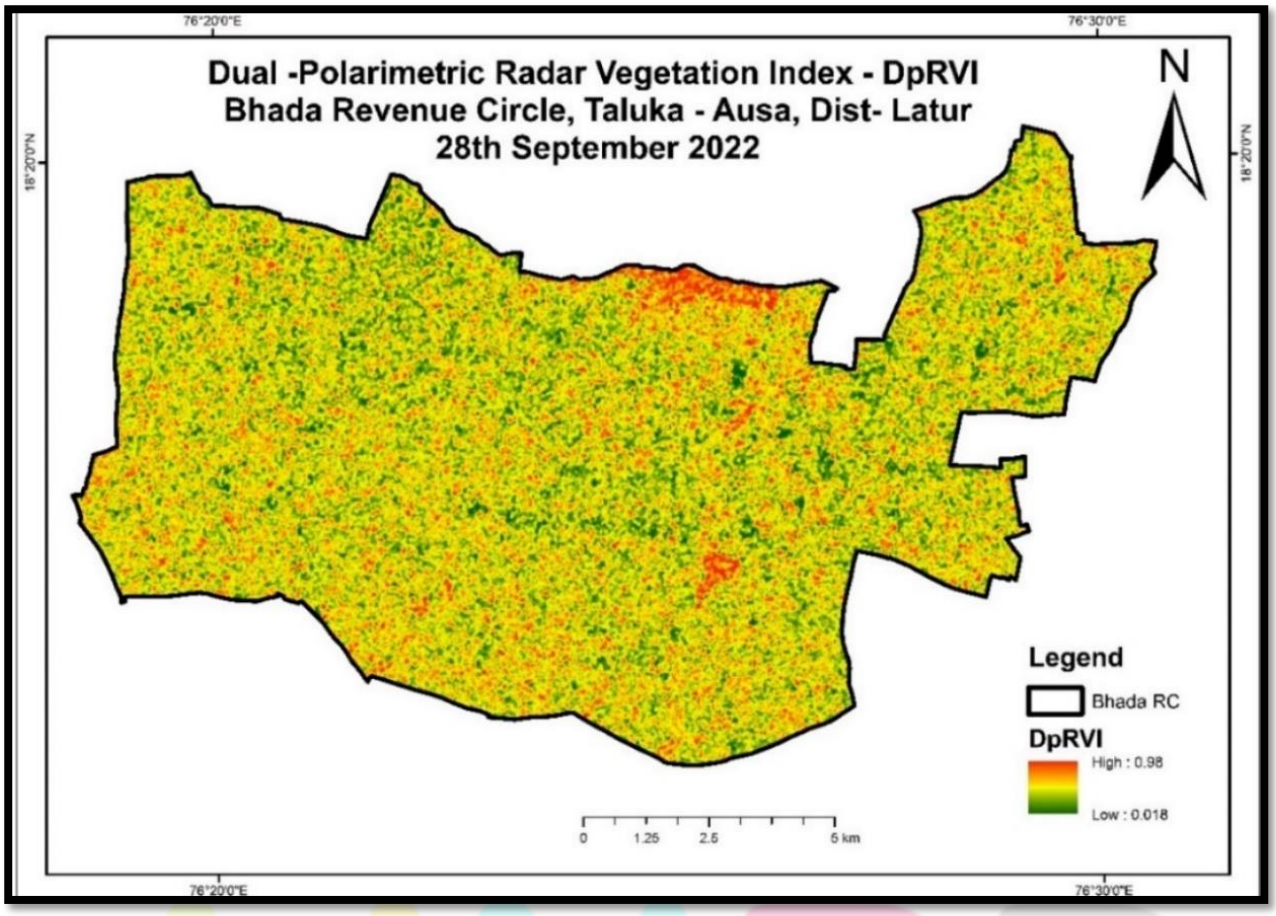

fig 5: Dual-pol radar vegetation index for Bhada Revenue Circle (DpRVI)

4.3 Plant Area Index (PAI)

The plant area index (PAI) represents the aggregated leaf and woody plant parts, such as stems, twigs, and fine branches, according to Macfarlane et al. (2007) and Zhao et al. (2011). Images of the canopy's cover and PAR readings above and below the canopy are used to directly compute the PAI, which may then be used to calculate the proportion of PAR transmitted through the canopy. Furthermore, the Plant Area Index assists in determining crop phenological transition dates.

4.4 Vegetation Water Content (VWC)

Vegetation water content (VWC) is expressed in 0 to 1. It is an essential biophysical aspect of plant health, and its estimate may be used to monitor vegetation water stress in real time.

4.5 Normalized Difference Vegetation Index (NDVI)

NDVI is a widely used index for assessing vegetation health and density. It measures the difference between near-infrared (NIR) and red (R) reflectance. NDVI is used to assess vegetation health and density

The formula for NDVI is: NDVI = (NIR - R) / (NIR + R).

4.6 Land Surface Water Index (LSWI)

LSWI is used to detect the presence of water bodies on the land surface. It operates based on the principle that water absorbs energy at near-infrared wavelengths and reflects energy at shortwave-infrared wavelengths. LSWI primarily focuses on identifying the presence of water on the land surface

The formula for LSWI is: LSWI = (NIR - SWIR) / (NIR + SWIR).

For this research, we derived biophysical parameters using Google Earth Engine and coding techniques, specifically for selected plots of soybean crop. These plots were obtained from the Croptech Pro mobile application. In collaboration with Semantic Technologies and Agritech Services Pune, these 62 soybean plots from the Bhada revenue circle in Latur district were carefully selected. These plots were not only registered but also geotagged within the Croptech Pro mobile application. This application provided valuable crop information, including details such as farmer names, survey numbers, and crop inventory data.

With this rich dataset in hand, which enabled us to calculate several biophysical parameters, including DpRVI, PAI, VWC, NDVI, and LSWI, for the selected plots. These parameters were derived to assess and monitor crop growth performance at various phenological growth stages.

This comprehensive approach allowed us to analyze and understand the dynamics of soybean crop growth, leveraging both remote sensing data from Google Earth Engine and ground-truth information from the Croptech Pro mobile application.

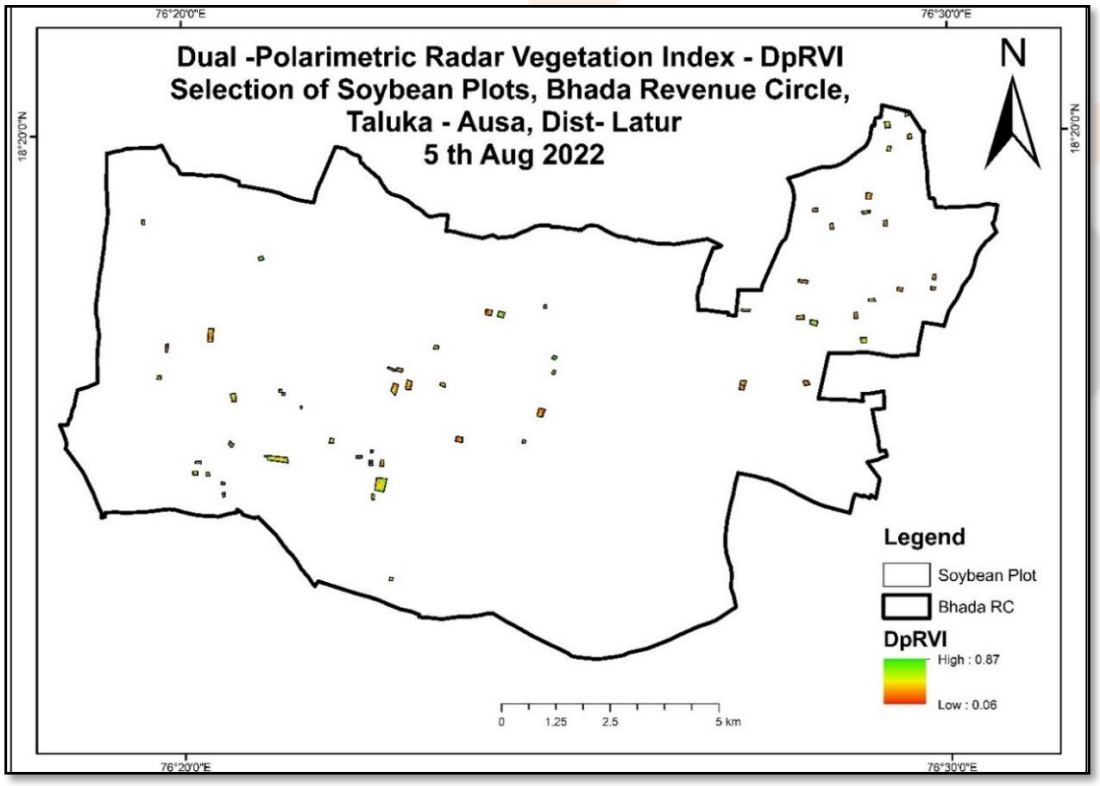

Fig 6: Map of selection of Soybean plots through Croptech PRO mobile application for derivation of DpRVI and Biophysical parameters.

5. Results and Discussions

5.1 Soybean and Dual Polarimetric Radar Vegetation Index (DpRVI)

Soybean (Glycine max) cultivation in Maharashtra occurs in kharif seasons. The kharif season runs from June to October. Soybean is known for its specific canopy architectural characteristics, particularly its bushy and random canopy structure after maturity, which consists of trifoliate leaves. In this study, we focused on the kharif season of 2022 in the Bhada revenue circle of Latur district

The developmental stages of soybean can be broadly categorized into two types: vegetative and reproductive stages. Within the vegetative stages, the emergence stage occurs within 1 to 10 days after sowing. The data from the government of Maharashtra indicated that the average sowing date ranged from June 13th to 20th. During this period, the DpRVI showed the lowest values. As the crop progressed through stages such as cotyledon (DAS 10 to 15), first trifoliate (DAS 15 to 17), second trifoliate (DAS 17 to 20), and V3 – V(n) (DAS 20 to 35), there was a gradual increase in DpRVI values.

In the reproductive stages, when flowering began (DAS 30-35), DpRVI values started to decrease. This decline continued through stages like full bloom (DAS 40-45), beginning pod (DAS 45-50), full pod (DAS 50-55), beginning seed (DAS 55-60), and full seed (DAS 60-70), where DpRVI reached a plateau condition. Subsequently, from the beginning of maturity (DAS 70-80) to full maturity (DAS 80 to 90-100), there was a notable decline in DpRVI values. This decrease in DpRVI was particularly evident between October 3rd and 10th when soybean was ready for harvest.

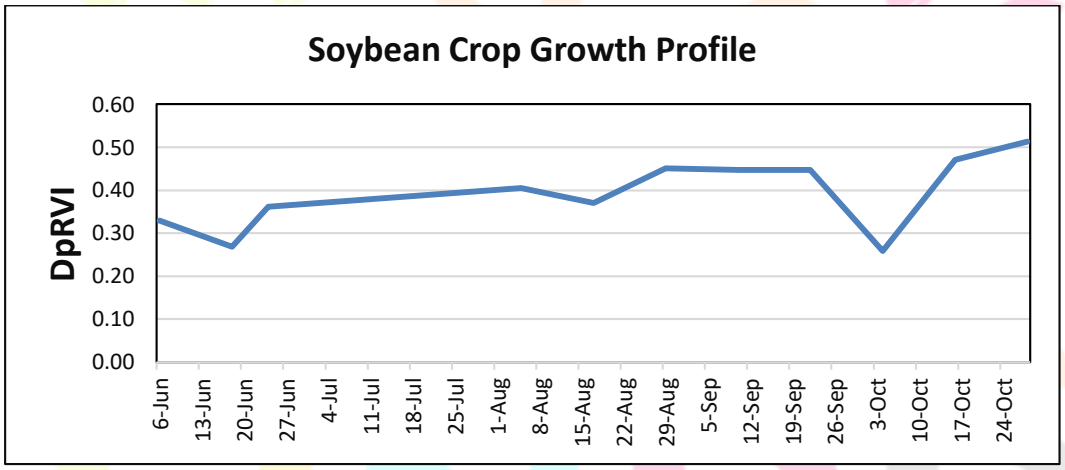

Fig 7 Soybean crop growth profile for showing DpRVI

In this study, we examined three specific plots in the Bhada revenue circle, registered within the Croptech Pro mobile application and featuring comprehensive crop inventory data, including farmer names and survey numbers. These plots were selected randomly, and we present the derived DpRVI for each of them in Figures 8 and 9, 11 and 12, and 14 and 15. These plots, labeled as 36, 39/42 and 85/A, exhibited DpRVI values ranging from 0.3 to 0.7, 0.1 to 0.7, and 0.1 to 0.8, respectively. This DpRVI data allowed us to interpret the crop growth conditions throughout the season (June to October in Maharashtra) for these individual plots, considering their spectral, spatial, and temporal characteristics at different phenological growth stages. This information provides valuable insights into the health and development of the soybean crop in each plot.

Based on the observations from this study, we enabled that the DpRVI has the potential to be employed for precision farming and providing crop advice to farmers. It enables the tracking of crop vegetation dynamics for crop growth monitoring on an individual basis, which can improve farm management, aid in crop disease management, and assist in irrigation scheduling and other farming practices.

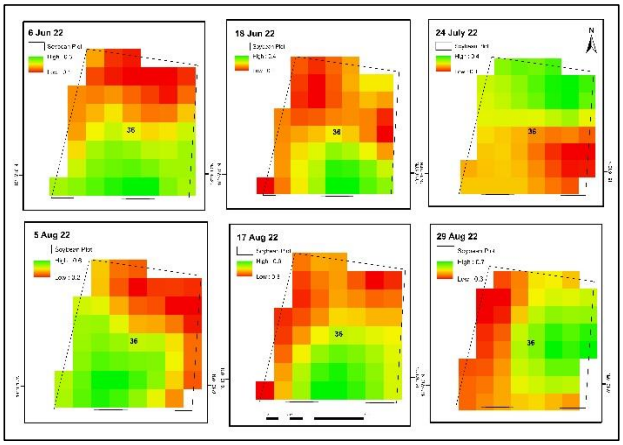

Fig 8 Temporal variations of plot no 36

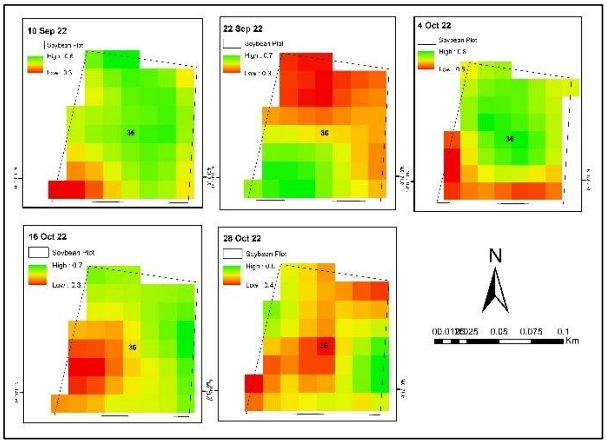

Fig 9 Temporal variations of plot no 36

Dates	Growth Stages	DpRVI Plot 36		
		Minimum	Maximum	Optimum
06-Jun	Pre DAS	0.1	0.3	0.2
18-Jun	VE Emergence	0.2	0.4	0.3
24-Jul	V1 Vegetative Trifoliate	0.1	0.4	0.25
05-Aug	V6 Vegetative Trifoliate	0.2	0.6	0.4
17-Aug	Full Pod Formation	0.3	0.6	0.45
29-Aug	Beginning Seed	0.3	0.7	0.5
10-Sep	Full Seed	0.3	0.6	0.45
22-Sep	Beginning Maturity	0.3	0.7	0.5
04-Oct	Full Maturity	0.5	0.8	0.65
16-Oct	Harvest	0.3	0.7	0.5

Fig 10 Table of Temporal variations of plot no 36

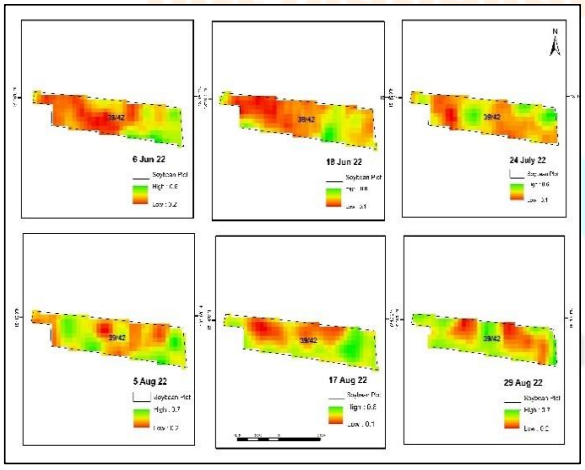

Fig 11 Temporal variations of plot no 39/42

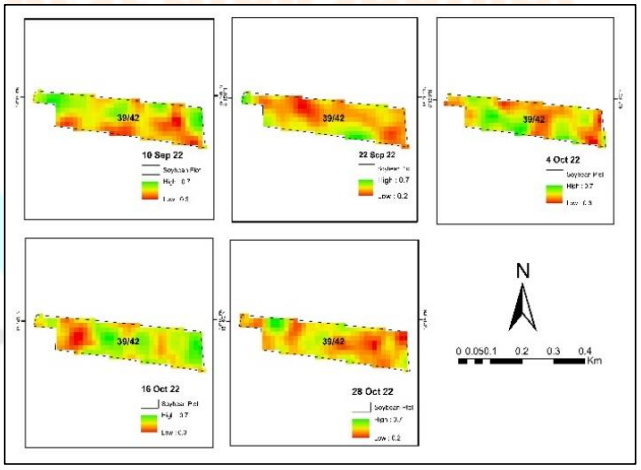

Fig 12 Temporal variations of plot no 39/42

Dates	Growth Stages	DpRVI Plot 39/42		
		Minimum	Maximum	Optimum
06-Jun	Pre DAS	0.2	0.6	0.4
18-Jun	VE Emergence	0.1	0.6	0.35
24-Jul	V1 Vegetative Trifoliate	0.1	0.6	0.35

05-Aug	V6 Vegetative Trifoliate	0.2	0.7	0.45
17-Aug	Full Pod Formation	0.1	0.6	0.35
29-Aug	Beginning Seed	0.2	0.7	0.45
10-Sep	Full Seed	0.3	0.7	0.5
22-Sep	Beginning Maturity	0.2	0.7	0.45
04-Oct	Full Maturity	0.3	0.7	0.5
16-Oct	Harvest	0.3	0.7	0.5

Fig 13 Table of temporal variations of plot no 39/42

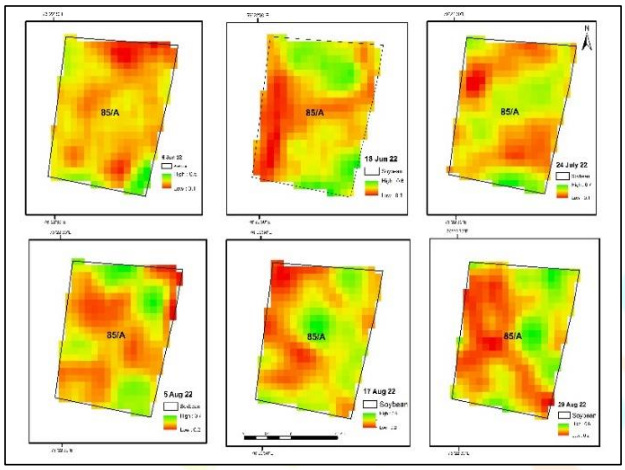

Fig 14 Temporal variations of plot no 85/A

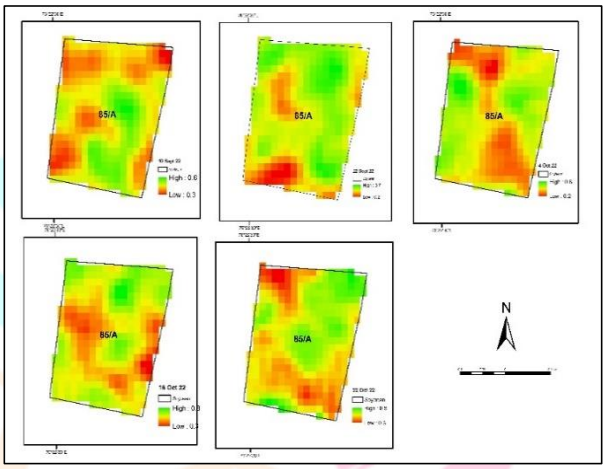

Fig 15 Temporal variations of plot no 85/A

Dates	Growth Stages	DpRVI Plot 85/ A		
		Minimum	Maximum	Optimum
06-Jun	Pre DAS	0.1	0.5	0.3
18-Jun	VE Emergence	0.1	0.6	0.35
24-Jul	V1 Vegetative Trifoliate	0.1	0.7	0.4
05-Aug	V6 Vegetative Trifoliate	0.2	0.7	0.45
17-Aug	Full Pod Formation	0.2	0.6	0.4
29-Aug	Beginning Seed	0.2	0.6	0.4
10-Sep	Full Seed	0.3	0.6	0.45
22-Sep	Beginning Maturity	0.2	0.7	0.45
04-Oct	Full Maturity	0.2	0.8	0.5
16-Oct	Harvest	0.3	0.8	0.55

Fig 16 Table of temporal variations of plot no 85/A

5.2 Crop Biophysical Parameters

In this research we use biophysical parameters for crop growth monitoring which plays an important role in the season monitoring of soybean crop. PAI, VWC, and NDVI and LSWI are an indicator that plays an important role in crop growth monitoring and season monitoring of crop. Correlation of biophysical parameters with DpRVI can be used for monitoring crop growth conditions.

Date	DPRVI	PAI	VWC	LSWI	NDVI	Growth Stages
06-Jun	0.34	0.37	-0.01	0.04	0.045	Day Before Sowing
18-Jun	0.33	0.14	0.05	0.07	0.015	VE Emergence
24-Jul	0.36	0.04	0.14	0.07	0.015	V1 Vegetative Trifoliate
05-Aug	0.42	0.37	0.08	0.16	0.014	V6 Vegetative Trifoliate
17-Aug	0.42	0.33	0.24	0.16	0.014	Full Pod Formation
29-Aug	0.45	0.69	0.21	0.18	0.015	Beginning Seed
10-Sep	0.53	0.92	0.14	0.18	0.140	Full Seed
22-Sep	0.54	0.94	0.11	0.13	0.149	Beginning Maturity
04-Oct	0.51	0.90	0.13	0.21	0.130	Full Maturity
16-Oct	0.53	0.59	0.12	0.12	0.015	Harvest

Fig 17 Table of Comparison between DpRVI and other biophysical variables

The DpRVI values for each field constantly increase as the vegetation growth increases from the emergence to the development stage to the beginning of pod development.

The observations presented in Figure 17 are based on the season average of the DpRVI and other biophysical parameters derived from 62 selected plots monitored through the Croptech Pro mobile application. These observations provided a comprehensive understanding of how these parameters change and evolve throughout the kharif season. Figure 17 likely illustrates how the average values of DpRVI, as well as other biophysical parameters such as PAI, VWC, LSWI, and NDVI, vary over the course of the growing season. By taking season averages with normalizes all indices. it's possible to identify trends and patterns in crop growth and health.

Additionally, Figure 18 presents a graphical representation that visually compares the temporal changes of DpRVI and the other biophysical parameters during the Kharif season. This comparison helped highlight correlations, fluctuations, and critical growth stages in the soybean crop. These graphical representations are valuable for gaining insights into how these parameters interact and influence each other over time, providing valuable information for crop monitoring and management decisions.

06-Jun (Day Before Sowing): just before sowing, the DpRVI is 0.34, indicating very limited vegetation. PAI is 0.37, suggesting a low plant canopy. VWC is -0.01, possibly indicating dry conditions. LSWI is 0.04, and the NDVI is 0.045, both of which indicate minimal vegetation. This corresponds to the "Day Before Sowing" stage.

18-Jun (VE Emergence): By this date, after emergence, DpRVI remains low at 0.33, but there's an increase in PAI (0.14), suggesting the beginning of plant growth. VWC also increases to 0.05, indicating improved moisture levels. LSWI and NDVI also show slight increases. This corresponds to the "VE Emergence" (Vegetative Emergence) stage.

24-Jul (V1 Vegetative Trifoliate): The crop has progressed to the "V1 Vegetative Trifoliate" stage. DpRVI remains steady at 0.36, while PAI and VWC continue to increase, indicating more developed vegetation. LSWI and NDVI also show slight increases.

05-Aug (V6 Vegetative Trifoliate): At the "V6 Vegetative Trifoliate" stage, DpRVI increases to 0.42, indicating healthier vegetation. PAI is 0.37, VWC is 0.08, LSWI is 0.16, and NDVI is 0.014, all suggesting continued growth.

17-Aug (Full Pod Formation): The "Full Pod Formation" stage sees DpRVI holding at 0.42, indicating stable vegetation. PAI and VWC are 0.33 and 0.24, respectively, suggesting a more developed crop canopy. LSWI and NDVI also show slight increases.

29-Aug (Beginning Seed): By the "Beginning Seed" stage, DpRVI has increased to 0.45, reflecting robust vegetation. PAI is notably higher at 0.69, indicating a dense plant canopy. VWC is 0.21, LSWI is 0.18, and NDVI is 0.015, further supporting healthy crop growth.

10-Sep (Full Seed): At "Full Seed," DpRVI continues to rise to 0.53, confirming vigorous vegetation. PAI is 1.05, showing a well-developed plant canopy. VWC is 0.14, LSWI is 0.18, and NDVI is 0.140, indicating advanced growth stages.

22-Sep (Beginning Maturity): The "Beginning Maturity" stage sees DpRVI at 0.54, with PAI at 0.94, suggesting a mature plant canopy. VWC is 0.11, LSWI is 0.13, and NDVI is 0.149, indicating the start of the maturity phase.

04-Oct (Full Maturity): By "Full Maturity," DpRVI is 0.51, with PAI at 0.90, indicating a mature crop. VWC is 0.13, LSWI is 0.21, and NDVI is 0.130, suggesting the peak of maturity.

16-Oct (Harvest): Finally, at the "Harvest" stage, DpRVI remains high at 0.53, but PAI decreases to 0.59 as the crop is harvested. VWC, LSWI, and NDVI values all decrease, indicating the end of the crop's growth cycle.

These observations demonstrate the progression of soybean crop growth and development throughout various phenological stages, with DpRVI and other parameters providing insights into the crop's health and maturity.

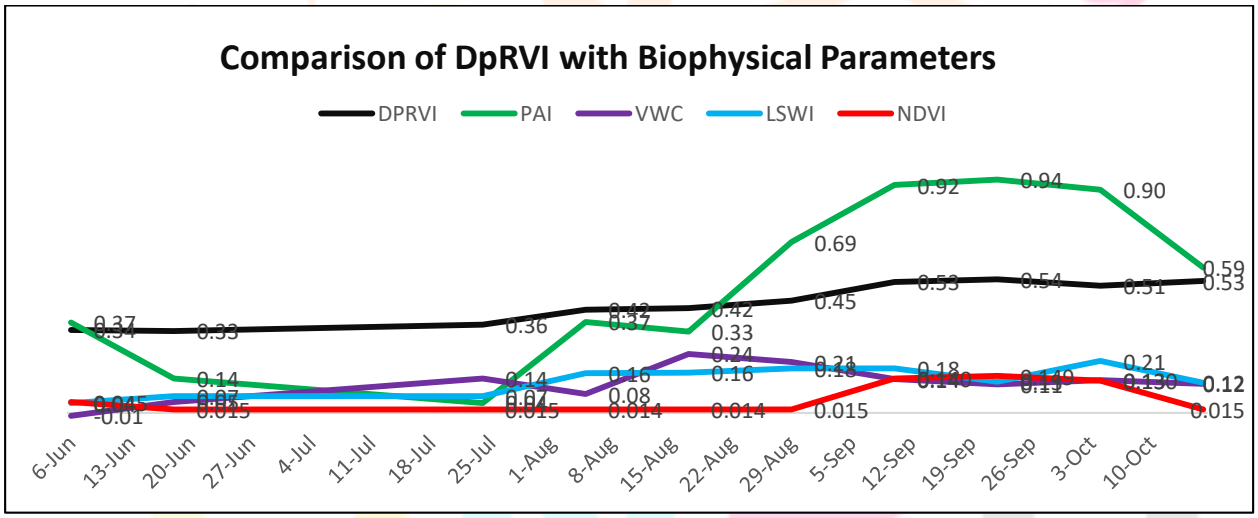

Fig 18 Comparison of DpRVI with Biophysical Parameters

In Figure 18, we conducted a comparative analysis of DpRVI with various biophysical parameters. To assess the effectiveness of using DpRVI to estimate biophysical parameters, we employed a linear regression model for cross-validation. This analysis aimed to evaluate the relationship between DpRVI and specific crop physical parameters, including the determination coefficient (R2) for DpRVI in relation to PAI, VWC, NDVI, and LSWI, resulting in an R2 value of 0.85.

Notably, the analysis revealed that DpRVI displayed the strongest correlation with the plant area index (PAI) and a moderate correlation with VWC, NDVI, and LSWI. These findings are graphically represented in Figure 17, which showcases the ranges of these biophysical parameters concerning DpRVI. These observations were aligned with specific dates corresponding to satellite data acquisition for soybean crops.

Furthermore, we conducted a multiple regression analysis involving DpRVI and the other biophysical parameters (i.e., PAI, VWC, NDVI, and LSWI), resulting in an R2 value of 0.85, as depicted in Figure 19.

However, it's crucial to acknowledge that while these findings indicate strong relationships between DpRVI and certain biophysical parameters, it may not be appropriate to assert that all biophysical parameters hold equal significance in predicting crop growth during crop monitoring. The importance of these parameters can indeed vary significantly, as observed in our study. We noted spatial and temporal variability in these parameters, influenced by different cropping patterns in various study areas. This underscores the need for careful consideration of the specific context and conditions when interpreting the significance of each biophysical parameter in crop growth monitoring.

Regression Statistics	
Multiple R	0.92
R Square	0.85
Adjusted R Square	0.75
Standard Error	0.042
Observations	62

Fig 19: Correlation regression analysis between vegetation index (DpRVI) and Crop Physical parameters i.e. Plant area index (PAI), vegetation water content (VWC), Normalized difference vegetation index (NDVI) and Land surface water index for Soybean with linear regression.

6. Limitations

In this study, we selected a Bhada revenue circle, Latur district in Maharashtra as our study area, we found some limitations which are mentioned as follows:

1. Fragmentation of land in Maharashtra.
2. Small land holdings of farmers.
3. Intercropping in cropping patterns in major crops like Soybean- cotton
4. Trap trees, large canopy trees, forest trees, orchard like plantation of teak plants are present in farms, so spectral signatures can be differed and may be affected by values in the index or other parameters

7. Benefits

1. Synthetic Aperture Radars (SARs) use microwave frequencies to broadcast and receive energy. The response recorded by these sensors is substantially determined by the target's structure and dielectric characteristics.
2. The structure of a canopy varies per crop and changes as the crop grows. SARs respond very well to structural variations, allowing them to properly identify crop types and to be sensitive to numerous crop biophysical factors (PAI, VWC, NDVI, LSWI).
3. Although optical sensors have traditionally been used for crop monitoring, advances in SAR application research, combined with the availability of SAR data at various frequencies and polarizations, have increased the profile of these sensors for agricultural monitoring.
4. "all-weather" capabilities of SARs make them useful in a variety of situations.

8. Conclusion

This study focused on experimenting with the Dual Polarimetric Radar Vegetation Index (DpRVI) derived from σVH0 / σVV0 data for Soybean crops. The index is based on the degree of polarization (m) and the dominant normalized eigenvalue (β = λ1/ Span) obtained from the 2 × 2 covariance matrix. Our particular emphasis was on tracking the phenological growth stages of Soybean crops and their relationship with independent biophysical variables: Plant Area Index (PAI), Vegetation Water Content (VWC), Normalized Difference Vegetation Index (NDVI), and Land Surface Water Index (LSWI), all in relation to the dependent variable, DpRVI.

Significant correlations were observed between these biophysical parameters and the Dual Polarimetric Radar Vegetation Index (DpRVI). DpRVI played a crucial role in assessing temporal variations in crop growth monitoring, predicting crop health, and monitoring overall crop development. We were able to describe the time series data, emphasizing each crop's phenological stage. Linear regression statistical analysis allowed us to quantify the relationship between PAI, VWC, and NDVI with DpRVI.

We found that Sentinel-1A data, with its 6-day revisit period, proved highly valuable for crop health monitoring, particularly during the kharif season when heavy cloud cover often obscures optical data.

In the context of India's population growth challenge and the need to increase the productivity to double farmers' income, the government has established a committee to support this goal, which is closely linked to crop yield and production. Hence, accurate crop monitoring, which measures and assesses crop yields, is of paramount importance.

The study's results indicates that using dual-polarimetric radar data enhances the accuracy of crop monitoring compared to single-polarization data. Furthermore, it underscores the significance of selecting an appropriate vegetation index capable of effectively capturing changes in crop growth dynamics. Overall, the utilization of Sentinel-1 SAR data and dual-polarimetric vegetation indices proves to be a valuable tool for crop monitoring and management, offering essential insights for crop yield estimation, crop mapping, and early detection of crop stress or damage. However, it's crucial to acknowledge that this approach has its limitations, and further research is necessary to fully comprehend its potential and constraints across various agricultural systems and environments.

Disclosures

No potential conflict of interest is reported by the authors.

Acknowledgment

The authors would take a moment to thank Semantic Technologies and Agritech Services Private Limited, Pune as the analysis was carried out under them. The Collection of Ground Truth data under field team members of Semantic Technologies and Agritech Services Private Limited, Pune.

Further, we would like to mention my vote of thanks to Dr. Dipankar Mandal who explained and discussed new trends in SAR data, his help in this project is really appreciated. Finally, we are grateful to the data provided by ESA Copernicus for providing Sentinel 1 data.

We express our sincere thanks to Mr. Sairam Iyer, Mr. Suryanarayan Dash, Mr. Pradip Patil and Mr. Kiran Prajapati for invaluable guidance, mentorship, and insightful inputs throughout the course of this project.

8. Link for Croptech PRO Mobile Application powered by Semantic Technologies and Agritech Services Pune

https://play.google.com/store/apps/details?id=com.croptechpro

9. References

[1] Dipankar Mandal, , Vineet Kumara,b , Debanshu Rathaa , Subhadip Deya , Avik Bhattacharya, Juan M. Lopez-Sanchezc , Heather McNairnd , Yalamanchili S. Raoa , Dual polarimetric radar vegetation index for crop growth monitoring using sentinel-1 SAR data. https://sentinels.copernicus.eu/web/sentinel/user-guides/sentinel-1-sar/product-types-processing-levels/level-1.

[2] Dipankar Mandal, Divya Sekhar Vaka1, Narayana Rao Bhogapurapu1, V. S. K. Vanama, Vineet Kumar, Y. S. Rao, Avik Bhattacharya, Sentinel-1 SLC preprocessing workflow for polarimetric applications: A generic practice for generating dual-pol covariance matrix elements in the SNAP S-1 toolbox**.**

[3] D. Mandal, V. Kumar, A. Bhattacharya, Y. S. Rao, P. Siqueira, and S. Bera, "Sen4Rice: A processing chain for differentiating early and late transplanted rice using time-series Sentinel-1 SAR data with Google Earth engine," IEEE Geoscience and Remote Sensing Letters, vol. 15, no. 12, pp. 1947–1951, 2018.

[4] D. Mandal, V. Kumar, A. Bhattacharya, Y. S. Rao, P. Siqueira, and S. Bera, "Sen4Rice: A processing chain for differentiating early and late transplanted rice using time-series Sentinel-1 SAR data with Google Earth engine," IEEE Geoscience and Remote Sensing Letters, vol. 15, no. 12, pp. 1947–1951, 2018

[5] J. M. Lopez-Sanchez, J. D. Ballester-Berman, and I. Hajnsek, "First results of rice monitoring practices in Spain by means of time series of TerraSAR-X dual-pol images," IEEE Journal of selected topics in applied earth observations and remote sensing, vol. 4, no. 2, pp. 412–422, 2010.

[6] D. Bargiel, "A new method for crop classification combining time series of radar images and crop phenology information," Remote sensing of environment, vol. 198, pp. 369–383, 2017.

[7] T. L. Ainsworth, J. Kelly, and J.-S. Lee, "Polarimetric analysis of dual polarimetric SAR imagery," in 7th European Conference on Synthetic Aperture Radar, 2008, pp. 1–4.

[8] A. Veloso et al., "Understanding the temporal behavior of crops using Sentinel-1 and Sentinel-2-like data for agricultural applications," Remote Sensing of Environment, vol. 199, pp. 415–426, 2017. .

[9] D. Bargiel, "A new method for crop classification combining time series of radar images and crop phenology information," Remote sensing of environment, vol. 198, pp. 369–383, 2017.

[10] S. Plank, "Rapid damage assessment by means of multi-temporal SAR—A comprehensive review and outlook to Sentinel-1," Remote Sensing, vol. 6, no. 6, pp. 4870–4906, 2014.

[11] Z. Malenovskỳ et al., "Sentinels for science: Potential of Sentinel-1,-2, and-3 missions for scientific observations of ocean, cryosphere, and land," Remote Sensing of Environment, vol. 120, pp. 91–101, 2012.

[12] Arias, M., Campo-Bescos, M.A., Alvarez-Mozos, J., 2020. Crop classification based on temporal signatures of Sentinel-1 observations over Navarre province, Spain. Remote Sens. 12 (2) URL. https://www.mdpi.com/2072-4292/12/2/278. Barakat, R., 1977. Degree of polarization and the principal idempotents of the coherency matrix. Opt. Commun. 23 (2), 147–150.

[13] Bhuiyan, H.A., McNairn, H., Powers, J., Friesen, M., Pacheco, A., Jackson, T.J., Cosh, M.H., Colliander, A., Berg, A., Rowlandson, T., et al., 2018. Assessing SMAP soil moisture scaling and retrieval in the carman (Canada) study site. Vadose Zone J. 17 (1).

[14] Bousbih, S., Zribi, M., Lili-Chabaane, Z., Baghdadi, N., El Hajj, M., Gao, Q., Mougenot, B., 2017. Potential of Sentinel-1 radar data for the assessment of soil and cereal cover parameters. Sensors 17 (11), 2617.

[15] Canisius, F., Shang, J., Liu, J., Huang, X., Ma, B., Jiao, X., Geng, X., Kovacs, J.M., Walters, D., 2018. Tracking crop phenological development using multi-temporal polarimetric Radarsat-2 data. Remote Sens. Environ. 210, 508–518.

[16] Chang, J., Shoshany, M., 2017. Radar polarization and ecological pattern properties across Mediterranean-to-arid transition zone. Remote Sens. Environ. 200, 368–377.

[17] Chang, J.G., Shoshany, M., Oh, Y., 2018. Polarimetric radar vegetation index for biomass estimation in desert fringe ecosystems. IEEE Trans. Geosci. Remote Sens. 56 (12), 7102–7108.

[18] Chipanshi, A., Zhang, Y., Kouadio, L., Newlands, N., Davidson, A., Hill, H., Warren, R., Qian, B., Daneshfar, B., Bedard, F., et al., 2015. Evaluation of the Integrated Canadian Crop Yield Forecaster (ICCYF) model for in-season prediction of crop yield across the Canadian agricultural landscape. Agric. For. Meteorol. 206, 137–150.

[19] Davidson, A., Fisette, T., Mcnairn, H., Daneshfar, B., 2017. Detailed crop mapping using D. Mandal, et al. Remote Sensing of Environment 247 (2020) 111954 16 remote sensing data (crop data layers). In: Delincé, J. (Ed.), Handbook on Remote Sensing for Agricultural Statistics. Global Strategy to improve Agricultural and Rural Statistics (GSARS), Rome, pp. 91–129 Ch. 4.

[20] De Bernardis, C.G., Vicente-Guijalba, F., Martinez-Marin, T., Lopez-Sanchez, J.M., March 2015. Estimation of key dates and stages in rice crops using dual-polarization SAR time series and a particle filtering approach. IEEE J. Select. Topics Appl. Earth Observ. Rem. Sens. 8 (3), 1008–1018.

[21] Denize, J., Hubert-Moy, L., Betbeder, J., Corgne, S., Baudry, J., Pottier, E., 2019. Evaluation of using Sentinel-1 and-2 time-series to identify winter land use in agricultural landscapes. Remote Sens. 11 (1), 37.

[22] ESA, 2015. User Guides - Sentinel-1 SAR. URL. https://sentinel.esa.int/web/sentinel/ user-guides/sentinel-1-sar/acquisition-modes/interferometric-wide-swath.

[23] ESA, 2017. Sen4CAP - Sentinels for Common Agriculture Policy. URL. http://esasen4cap.org/. Fehr, W., Caviness, C., Burmood, D., Pennington, J., 1971. Stage of development descriptions for soybeans, Glycine Max (L.) Merrill 1. Crop Sci. 11 (6), 929–931. [24] Fikriyah, V.N., Darvishzadeh, R., Laborte, A., Khan, N.I., Nelson, A., 2019. Discriminating transplanted and direct seeded rice using Sentinel-1 intensity data. Int. J. Appl. Earth Obs. Geoinf. 76, 143–153.

[25] Gururaj, P., Umesh, P., Shetty, A., 2019. Assessment of spatial variation of soil moisture during maize growth cycle using SAR observations. In: Remote Sensing for Agriculture, Ecosystems, and Hydrology XXI. 11149. International Society for Optics and Photonics, pp. 1114916.

[26] Inglada, J., Vincent, A., Arias, M., Marais-Sicre, C., 2016. Improved early crop type identification by joint use of high temporal resolution SAR and optical image time series. Remote Sens. 8 (5), 362.

[27] Jia, M., Tong, L., Zhang, Y., Chen, Y., 2013. Multitemporal radar backscattering measurement of wheat fields using multifrequency (L, S, C, and X) and full-polarization. Radio Sci. 48 (5), 471–481.

[28] Khabbazan, S., Vermunt, P., Steele-Dunne, S., Ratering Arntz, L., Marinetti, C., van der Valk, D., Iannini, L., Molijn, R., Westerdijk, K., van der Sande, C., 2019. Crop monitoring using Sentinel-1 data: a case study from the Netherlands. Remote Sens. 11 (16), 1887.

[29] Kim, Y., van Zyl, J.J., 2009. A time-series approach to estimate soil moisture using polarimetric radar data. IEEE Trans. Geosci. Remote Sens. 47 (8), 2519–2527.

[30] Kumar, P., Prasad, R., Gupta, D., Mishra, V., Vishwakarma, A., Yadav, V., Bala, R., Choudhary, A., Avtar, R., 2018. Estimation of winter wheat crop growth parameters using time series Sentinel-1A SAR data. Geocarto Int. 33 (9), 942–956.

[31] Kussul, N., Lemoine, G., Gallego, F.J., Skakun, S.V., Lavreniuk, M., Shelestov, A.Y., 2016. Parcel-based crop classification in Ukraine using Landsat-8 data and Sentinel-1A data. IEEE J. Select. Topics Appl. Earth Observ. Rem. Sens. 9 (6), 2500–2508.

[32] Lasko, K., Vadrevu, K.P., Tran, V.T., Justice, C., 2018. Mapping double and single crop paddy rice with Sentinel-1A at varying spatial scales and polarizations in Hanoi, Vietnam. IEEEJ. Select. Topics Appl. Earth Observ. Rem. Sens. 11 (2), 498–512.

[33] Lee, J.-S., Grunes, M.R., Pottier, E., 2001. Quantitative comparison of classification capability: fully polarimetric versus dual and single-polarization sar. IEEE Trans. Geosci. Remote Sens. 39 (11), 2343–2351.

[34] López-Lozano, R., Duveiller, G., Seguini, L., Meroni, M., Garca-Condado, S., Hooker, J., Leo, O., Baruth, B., 2015. Towards regional grain yield forecasting with 1 km-resolution EO biophysical products: strengths and limitations at pan-European level. Agric. For. Meteorol. 206, 12–32.

[35] Lopez-Sanchez, J.M., Vicente-Guijalba, F., Ballester-Berman, J.D., Cloude, S.R., May 2014. Polarimetric response of rice fields at C-band: analysis and phenology retrieval. IEEE Trans. Geosci. Remote Sens. 52 (5), 2977–2993.

[36] Mandal, D., Kumar, V., Bhattacharya, A., Rao, Y.S., Siqueira, P., Bera, S., 2018. Sen4Rice: a processing chain for differentiating early and late transplanted rice using timeseries Sentinel-1 SAR data with Google Earth engine. IEEE Geosci. Remote Sens. Lett. 15 (12), 1947–1951.

[37] Mandal, D., Kumar, V., McNairn, H., Bhattacharya, A., Rao, Y., 2019. Joint estimation of Plant Area Index (PAI) and wet biomass in wheat and soybean from C-band polarimetric SAR data. Int. J. Appl. Earth Obs. Geoinf. 79, 24-34.

[38] Mandal, D., Kumar, V., Lopez-Sanchez, J.M., Bhattacharya, A., McNairn, H., Rao, Y., 2020a. Crop biophysical parameter retrieval from Sentinel-1 SAR data with a multitarget inversion of Water Cloud Model. Int. J. Remote Sens. 41 (14), 5503–5524.

[39] Mandal, D., Kumar, V., Ratha, D., Lopez-Sanchez, J.M., Bhattacharya, A., McNairn, H., Rao, Y., Ramana, K., 2020b. Assessment of rice growth conditions in a semi-arid region of India using the Generalized Radar Vegetation Index derived from RADARSAT-2 polarimetric SAR data. Remote Sens. Environ. 237, 111561.

[40] Mandal, D., Ratha, D., Bhattacharya, A., Kumar, V., McNairn, H., Rao, Y.S., Frery, A.C., 2020c. A radar vegetation index for crop monitoring using compact polarimetric sar data. IEEE Trans. Geosci. Rem. Sens. https://doi.org/10.1109/TGRS.2020.2976661. McNairn, H., Shang, J., 2016. A review of multitemporal synthetic aperture radar (SAR) for crop monitoring. In: Multitemporal Remote Sensing. Springer, pp. 317–340.

[41] McNairn, H., Champagne, C., Shang, J., Holmstrom, D., Reichert, G., 2009. Integration of optical and Synthetic Aperture Radar (SAR) imagery for delivering operational annual crop inventories. ISPRS J. Photogramm. Remote Sens. 64 (5), 434–449.

[42] McNairn, H., Tom, J.J., Powers, J., BÃlair, S., Berg, A., Bullock, P., Colliander, A., Cosh, M.H., Kim, S.-B., Ramata, M., Pacheco, A., Merzouki, A., 2016. Experimental Plan SMAP Validation Experiment 2016 in Manitoba, Canada (SMAPVEX16-MB). URL. https://smap.jpl.nasa.gov/internal_resources/390/.

[43] McNairn, H., Jiao, X., Pacheco, A., Sinha, A., Tan, W., Li, Y., 2018. Estimating canola phenology using synthetic aperture radar. Remote Sens. Environ. 219, 196–205.

[44] Nasirzadehdizaji, R., Balik Sanli, F., Abdikan, S., Cakir, Z., Sekertekin, A., Ustuner, M., 2019. Sensitivity analysis of multi-temporal sentinel-1 SAR parameters to crop height and canopy coverage. Appl. Sci. 9 (4), 655.

[45] Nelson, A., Setiyono, T., Rala, A., Quicho, E., Raviz, J., Abonete, P., Maunahan, A., Garcia, C., Bhatti, H., Villano, L., et al., 2014. Towards an operational SAR-based rice monitoring system in Asia: examples from 13 demonstration sites across Asia in the RIICE project. Remote Sens. 6 (11), 10773–10812.

[46] Nguyen, D.B., Gruber, A., Wagner, W., 2016. Mapping rice extent and cropping scheme in the Mekong Delta using Sentinel-1A data. Rem. Sens. Lett. 7 (12), 1209–1218.

[47] Pacheco, A., McNairn, H., Li, Y., Lampropoulos, G., Powers, J., 2016. Using RADARSAT-2 and TerraSAR-X satellite data for the identification of canola crop phenology. In: Remote Sensing for Agriculture, Ecosystems, and Hydrology XVIII. 9998. International Society for Optics and Photonics, pp. 999802.

[48] Periasamy, S., 2018. Significance of dual polarimetric synthetic aperture radar in biomass retrieval: an attempt on Sentinel-1. Remote Sens. Environ. 217, 537–549.

[49] Raney, R.K., Cahill, J.T., Patterson, G.W., Bussey, D.B.J., 2012. The m-chi decomposition of hybrid dual-polarimetric radar data with application to lunar craters. J. Geophys. Res. 117 (E12).

[50] Shirvany, R., Chabert, M., Tourneret, J.-Y., 2012. Estimation of the degree of polarization for hybrid/compact and linear dual-pol SAR intensity images: principles and applications. IEEE Trans. Geosci. Remote Sens. 51 (1), 539–551.

[51] Singha, M., Dong, J., Zhang, G., Xiao, X., 2019. High resolution paddy rice maps in cloudprone Bangladesh and Northeast India using Sentinel-1 data. Scientific Data 6 (1), 26.

[52] Szigarski, C., Jagdhuber, T., Baur, M., Thiel, C., Parrens, M., Wigneron, J.-P., Piles, M., Entekhabi, D., 2018. Analysis of the radar vegetation index and potential improvements. Remote Sens. 10 (11), 1776.

[53] Touzi, R., Hurley, J., Vachon, P.W., 2015. Optimization of the degree of polarization for enhanced ship detection using polarimetric RADARSAT-2. IEEE Trans. Geosci. Remote Sens. 53 (10), 5403–5424.

[54] Touzi, R., Omari, K., Sleep, B., Jiao, X., 2018. Scattered and received wave polarization optimization for enhanced peatland classification and fire damage assessment using polarimetric PALSAR. IEEE J. Select. Topics Appl. Earth Observ. Rem. Sens. 11 (11), 4452–4477.

[55] Trudel, M., Charbonneau, F., Leconte, R., 2012. Using RADARSAT-2 polarimetric and ENVISAT-ASAR dual-polarization data for estimating soil moisture over agricultural fields. Can. J. Remote. Sens. 38 (4), 514–527.

[56] Ulaby, F., 1975. Radar response to vegetation. IEEE Trans. Antennas Propag. 23 (1), 36–45.

[57] Van Tricht, K., Gobin, A., Gilliams, S., Piccard, I., 2018. Synergistic use of radar Sentinel-1 and optical Sentinel-2 imagery for crop mapping: a case study for Belgium. Remote Sens. 10 (10), 1642.

[58] Veloso, A., Mermoz, S., Bouvet, A., Le Toan, T., Planells, M., Dejoux, J.-F., Ceschia, E., 2017. Understanding the temporal behavior of crops using Sentinel-1 and Sentinel-2- like data for agricultural applications. Remote Sens. Environ. 199, 415–426.

[59] Vreugdenhil, M., Wagner, W., Bauer-Marschallinger, B., Pfeil, I., Teubner, I., Rüdiger, C., Strauss, P., 2018. Sensitivity of Sentinel-1 backscatter to vegetation dynamics: an Austrian case study. Remote Sens. 10 (9), 1396.

[60] Wang, H., Magagi, R., Goita, K., 2016. Polarimetric decomposition for monitoring crop growth status. IEEE Geosci. Remote Sens. Lett. 13 (6), 870–874.

[61] Whelen, T., Siqueira, P., 2018. Time-series classification of Sentinel-1 agricultural data over North Dakota. Rem. Sens. Lett. 9 (5), 411–420.

[62] Wigneron, J.-P., Pardé, M., Waldteufel, P., Chanzy, A., Kerr, Y., Schmidl, S., Skou, N., 2004. Characterizing the dependence of vegetation model parameters on crop structure, incidence angle, and polarization at L-band. IEEE Trans. Geosci. Remote Sens. 42 (2), 416–425.

[63] Wiseman, G., McNairn, H., Homayouni, S., Shang, J., 2014. RADARSAT-2 polarimetric SAR response to crop biomass for agricultural production monitoring. IEEE J. Select. Topics Appl. Earth Observ. Rem. Sens. 7 (11), 4461–4471.

[64] de Wit, A., Duveiller, G., Defourny, P., 2012. Estimating regional winter wheat yield with WOFOST through the assimilation of green area index retrieved from MODIS observations. Agric. For. Meteorol. 164, 39–52.

[65] Wu, L.-K., Moore, R.K., Zoughi, R., 1985. Sources of scattering from vegetation canopies at 10 GHz. IEEE Trans. Geosci. Remote Sens. GE-23 (5), 737–745.